Disruption of the olivo-cerebellar circuit by Purkinje neuron-specific ablation of BK channels

Xiaowei Chen[a,1], Yury Kovalchuk[a,1], Helmuth Adelsberger[a], Horst A. Henning[a], Matthias Sausbier[b], Georg Wietzorrek[c], Peter Ruth[b], Yosef Yarom[d], and Arthur Konnerth[a,2]

[a]Center for Integrated Protein Science and Institute of Neuroscience, Technical University Munich, 80802 Munich, Germany; [b]Department of Pharmacology and Toxicology, University of Tübingen, D-72076 Tübingen, Germany; [c]Molecular and Clinical Pharmacology, Innsbruck Medical University, 6020 Innsbruck, Austria; and [d]Department of Neurobiology, Life Science Institute and the Interdisciplinary Center for Neural Computation, Hebrew University, Jerusalem 91904, Israel

Edited* by Rodolfo R. Llinas, New York University Medical Center, New York, NY, and approved April 22, 2010 (received for review February 11, 2010)

The large-conductance voltage- and calcium-activated potassium (BK) channels are ubiquitously expressed in the brain and play an important role in the regulation of neuronal excitation. Previous work has shown that the total deletion of these channels causes an impaired motor behavior, consistent with a cerebellar dysfunction. Cellular analyses showed that a decrease in spike firing rate occurred in at least two types of cerebellar neurons, namely in Purkinje neurons (PNs) and in Golgi cells. To determine the relative role of PNs, we developed a cell-selective mouse mutant, which lacked functional BK channels exclusively in PNs. The behavioral analysis of these mice revealed clear symptoms of ataxia, indicating that the BK channels of PNs are of major importance for normal motor coordination. By using combined two-photon imaging and patch-clamp recordings in these mutant mice, we observed a unique type of synaptic dysfunction in vivo, namely a severe silencing of the climbing fiber–evoked complex spike activity. By performing targeted pharmacological manipulations combined with simultaneous patch-clamp recordings in PNs, we obtained direct evidence that this silencing of climbing fiber activity is due to a malfunction of the tripartite olivo-cerebellar feedback loop, consisting of the inhibitory synaptic connection of PNs to the deep cerebellar nuclei (DCN), followed by a projection of inhibitory DCN afferents to the inferior olive, the origin of climbing fibers. Taken together, our results establish an essential role of BK channels of PNs for both cerebellar motor coordination and feedback regulation in the olivo-cerebellar loop.

cerebellar ataxia | climbing fiber | complex spike | two-photon imaging

The large-conductance voltage- and Ca^{2+}-activated K^+ (BK) channels, which modulate action potential firing by regulating the fast afterhyperpolarization (1), are highly expressed in cerebellar Purkinje neurons (PNs) (2, 3). Several in vitro studies demonstrated that BK channels in the somata and dendrites of PNs are activated by action potentials and, in turn, regulate the firing rate and firing pattern of these neurons (4–10). Furthermore, mice lacking BK channels exhibit clear symptoms of cerebellar ataxia (2), indicating a critical role of BK channels in motor control. On the cellular level, this total deletion of BK channels results in a marked reduction in action potential activity of PNs, which was suggested to be mediated by depolarization-induced inactivation of Na^+ channels (2). It should be noted, however, that not only PNs but also other cerebellar neurons, like Golgi cells, express BK channels and exhibit a change in firing properties in total BK channels–deficient mice (11). Therefore, it is difficult to evaluate the relative contribution of the modified PNs to the motor deficits of mice lacking BK channels.

The reduced activity of inhibitory PNs and the resultant hyperexcitability of their targets, the deep cerebellar nuclei (DCN), are considered to be important features of cerebellar ataxia (12, 13), but their impact on downstream brain circuits is largely unknown. It has been suggested that the olivo-cerebellar circuit, one of the major neuronal circuits for motor control in the brain, provides timing signals for motor coordination (14–16). This circuit is a loop of interconnected structures where the cerebellar cortex innervates the inferior olivary nucleus (IO) via the DCN, and the olivary neurons via the climbing fibers are fed back into the cerebellar cortex. Whereas the olivary neurons exert an excitatory action on the PN at the cerebellar cortex, both the PN and DCN terminals exert an inhibitory action on their target cells (17–19). Thus, it is likely that this long-range feedback loop will be affected by the alteration in PN's activity observed in the $BK^{-/-}$ mouse. For these reasons, the aims of the present study were to assess the specific role of BK channels of PNs for motor coordination and downstream circuit function in vivo.

Results and Discussion

BK Channels of Purkinje Neurons Are Essential for Motor Coordination. To explore the specific contribution of BK channels of PNs for motor behavior, we generated a mouse line lacking BK channels exclusively in PNs, which we refer to as PN-$BK^{-/-}$ (for details see *SI Materials and Methods*). The BK channel α-subunit in PNs was specifically ablated in mice by intercrossed constitutive heterozygous BK L1/+ mice (SV129 background) with transgenic mice expressing the Cre recombinase under the control of the Purkinje protein 2 gene (20). The resulting genotype was analyzed by PCR amplification and confirmed by immunohistochemistry as described previously (Fig. S1) (2, 20). Next we examined motor behavior in total $BK^{-/-}$ mice and in PN-$BK^{-/-}$ mice and compared it with that of WT mice. Consistent with a previous study (2), we observed a pronounced deficiency in motor coordination in total $BK^{-/-}$ mice by footprint analysis ($n = 4$ WT and 4 total $BK^{-/-}$ mice; $P < 0.05$) and by the increased number of slips of the hind limbs during either ladder runway ($n = 7$ WT and 4 total $BK^{-/-}$ mice; $P < 0.05$) or balance beam tests ($n = 6$ WT and 5 total $BK^{-/-}$ mice; in balance beam tests, total $BK^{-/-}$ mice were unable to move forward on the beam) (Fig. 1 *A* and *B*). In the same behavioral tests, PN-$BK^{-/-}$ mice also exhibited clear deficits in their walking behavior (total numbers of animals were 12 WT mice and 11 PN-$BK^{-/-}$ mice; $P < 0.05$ for each test) (Fig. 1 *C* and *D*). Remarkably, the behavioral deficits in PN-$BK^{-/-}$ mice were similar to those seen in the total $BK^{-/-}$ mice, albeit the severity of the symptoms was slightly reduced. These observations provide unambiguous support for the specific involvement of PN's BK channels in cerebellar motor control.

On the cellular level, previous experiments from brain slice recordings demonstrated a pronounced reduction in simple spike (SS) activity of PNs in $BK^{-/-}$ mice (2). Remarkably, many PNs of $BK^{-/-}$ mice had strongly depolarized resting membrane potentials, some exhibiting even a total depolarization blockade

Author contributions: Y.Y. and A.K. designed research; X.C., Y.K., H.A., H.A.H., M.S., G.W., P.R., and Y.Y. performed research; A.K. contributed new reagents/analytic tools; X.C., H.A., H.A.H., M.S., P.R., and A.K. analyzed data; and X.C., Y.Y., and A.K. wrote the paper.

The authors declare no conflict of interest.

*This Direct Submission article had a prearranged editor.

[1]X.C. and Y.K. contributed equally to this work.

[2]To whom correspondence should be addressed. E-mail: arthur.konnerth@lrz.tu-muenchen.de.

This article contains supporting information online at www.pnas.org/lookup/suppl/doi:10.1073/pnas.1001745107/-/DCSupplemental.

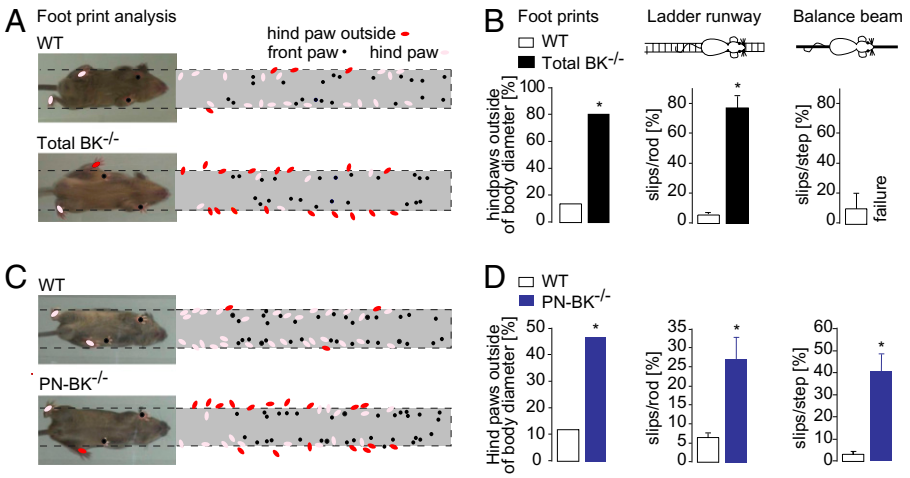

Fig. 1. Impairments of motor coordination in both total BK$^{-/-}$ and PN-BK$^{-/-}$ mice. (*A*) Footprint patterns in WT and total BK$^{-/-}$ mice. *Left:* Mice walking on a glass plate. Their body diameters are indicated by dotted lines. *Right:* Summary of the superimposed paw positions of four WT and four total BK$^{-/-}$ mice. (*B*) Bar chart comparison of walking behavior in WT and total BK$^{-/-}$ mice. *Left:* Summary of *A* showing the percentage of hindpaw positions outside of the body diameter. *Center:* Percentage of hindpaw slips relative to the total number of steps on a ladder (n = 7 WT and 4 total BK$^{-/-}$ mice). *Right:* Percentage of hindpaw slips during running on a balance beam (n = 6 WT and 5 total BK$^{-/-}$ mice). (*C*) Footprint patterns in WT and PN-BK$^{-/-}$ mice. *Right:* Summary of the paw positions of 7 WT and PN-BK$^{-/-}$ mice. (*D*) Histograms indicate the percentage of hindpaw positions outside of the body diameter (*Left:* summary of the number of red dots in *C*), the percentage of hindpaw slips relative to the total number of steps on a ladder runway (*Center*) (n = 12 WT and 11 PN-BK$^{-/-}$ mice), and the percentage of hindpaw slips during running on a balance beam (*Right*) (n = 9 WT and 9 PN-BK$^{-/-}$ mice). Failure means in this case that the animals are not able to move forward on the beam but fall down. *P < 0.05. Error bars show SEM.

(2, 11). These observations indicated that the cause for the reduction in SS activity is a partial inactivation of Na^+ channels, because of this excessive depolarization. To determine the SS firing rate in PN-BK$^{-/-}$ mice in vivo, we performed cell-attached patch-clamp recordings in fluorescently labeled PNs using the two-photon imaging-based "shadow patch" approach (21) under isoflurane anesthesia (Fig. S2*A*). The spontaneous activity in vivo consisted of two types of responses: the characteristic SSs, which reflect an interplay between afferent synaptic activity (22, 23) and intrinsic properties of PNs (24, 25); and the complex spikes (CSs) (26), which are generated by the activity of the climbing fibers (Fig. S2*B*). As in the previous studies (2), we observed a substantial decrease in SS frequency in PN-BK$^{-/-}$ mice, albeit to a lesser degree (Fig. S2 *C* and *D*). The mean frequency of SS for all cells was 1.2-fold higher in WT cells (67.0 ± 10.3 Hz; n = 34 cells and 10 mice) than in PN-BK$^{-/-}$ mice (55.6 ± 1.0 Hz; n = 57 cells and 10 mice; P < 0.05; Table S1), and approximately 2.7-fold higher than in total BK$^{-/-}$ mice (24.7 ± 3.5 Hz; n = 30 cells and 5 mice; P < 0.01). We conclude that PN-BK$^{-/-}$ mice are ataxic and display a reduction in SS activity. The results are in general agreement with the original suggestion that a "depolarization block" may underlie the reduced SS firing frequency (2). Together, our observations strongly support the role of PN's BK channels in motor coordination. However, comparison of the changes in total BK$^{-/-}$ mice with those in PN-BK$^{-/-}$ mice shows that the latter exhibit a lesser degree of severity. This implies that the motor impairment in total BK$^{-/-}$ mice is probably caused by the deletion of BK channels in both PNs and other cell types (e.g., Golgi cells) (11).

Severe Silencing of Climbing Fiber–Evoked CS in PN-BK$^{-/-}$ Mice in Vivo. The striking finding was a significant reduction up to complete elimination of CS activity in a large fraction of PNs (Fig. 2). Under our recording conditions, the climbing fiber–mediated CS activity could be unambiguously distinguished from the SS activity: first by the waveform of the electrical responses recorded in the cell-attached configuration (Fig. S2*B*, *Insets*), and second by the well-established fact that CSs, but not SSs, are associated with global dendritic Ca^{2+} transients (27) (Fig. 2*A*). For comparison of the changes in frequency of CS activity in the two genotypes, PNs were assigned to three frequency classes that were categorized as "normal" (>0.6 Hz), "quiet" (0.05–0.6 Hz) or "silent" (0–0.05 Hz) (Fig. 2 *A*–*C*). Unexpectedly, we found that the CS activity in PN-BK$^{-/-}$ mice was severely reduced, with a dramatic increase of silent PNs from virtually none in WT to 46% in PN-BK$^{-/-}$ mice and an increase of the quiet PNs from 5% to 23%. Silent, quiet, and normal PNs were randomly distributed within all regions of the cerebellar vermis. In line with these observations, the proportion of normal PNs dropped from 95% in WT to 31% in PN-BK$^{-/-}$ mice (n = 34 WT cells and 57 PN-BK$^{-/-}$ cells) (Fig. 2*C*). The significant decrease in CS activity was also seen in average firing rates for the quiet and normal categories, which were reduced from 0.45 ± 0.08 Hz in WT (n = 2 quiet cells out of a total of 34 cells) to 0.15 ± 0.03 Hz in PN-BK$^{-/-}$ mice (n = 13/57 quiet cells; P < 0.05) and from 1.45 ± 0.06 Hz in WT (n = 32 of 34 normal cells) to 1.07 ± 0.08 Hz in PN-BK$^{-/-}$ mice (n = 18 of 57 normal cells; P < 0.01; Table S1).

What are the mechanisms that might underlie the impaired CS activity? We first considered the possibility of breakdown of climbing fiber–PN synapses. Such a hypothetical breakdown may result from excessive release of endocannabinoids (28) in PN-BK$^{-/-}$ mice, due to depolarization of BK-deficient PNs (2). To test this possibility, we performed whole-cell recordings of climbing fiber–evoked responses in PNs of cerebellar slices using conventional stimulation procedures (29) (Fig. 2*D*). In agreement with a previous work indicating a rather modest role of BK channels in shaping the CS waveform (30), we noticed in PNs of PN-BK$^{-/-}$ mice a slight increase in the number of spikelets as compared with WT mice (mean number of spikelets = 3.3 ± 0.1 for WT cells and 4.1 ± 0.1 for PN-BK$^{-/-}$ cells; n = 5 cells for each genotype; P < 0.001) (Fig. S3 *A* and *B*). We also found that the climbing fiber–evoked dendritic Ca^{2+} transients had a larger amplitude and a slower time course in PN-BK$^{-/-}$ (Fig. S3 *C* and *D*). This increase in dendritic Ca^{2+} signal is consistent with a previous study reporting an increase in Ca^{2+} entry per action potential in the presence of a pharmacological blocker of BK channels (4). It is important to note that CSs could be elicited with the same high degree of reliability in both genotypes (5 of 5 cells in WT and 10 of 10 cells in PN-BK$^{-/-}$ mice) (Fig. 2*E*). We also tested the possibility that the synaptic failures in PN-BK$^{-/-}$ mice may occur only at higher frequencies of climbing fiber activity, as encountered under in vivo conditions. However, even prolonged climbing fiber stimulation at 1 Hz had no deleterious effect on CS activity in PN-BK$^{-/-}$ mice (Fig. S4). Together, these results indicate that the basic properties of climbing fiber–PN synapses were unaltered by the removal of BK channels in PN-BK$^{-/-}$ mice.

Disruption of the Olivo-Cerebellar Circuit in PN-BK$^{-/-}$ Mice. We next investigated whether the reduction in the frequency of CS activity could be due to malfunction of the olivo-cerebellar circuit. First we examined the integrity of the olivo-cerebellar connection by applying harmaline, a tremorgenic drug known to exert a rather specific action on the olivary nucleus (31) (Fig. 3*A*). The lack of harmaline action on CS activity through a direct effect on PNs was confirmed in control experiments, in which local application of harmaline to the recorded PNs did not significantly

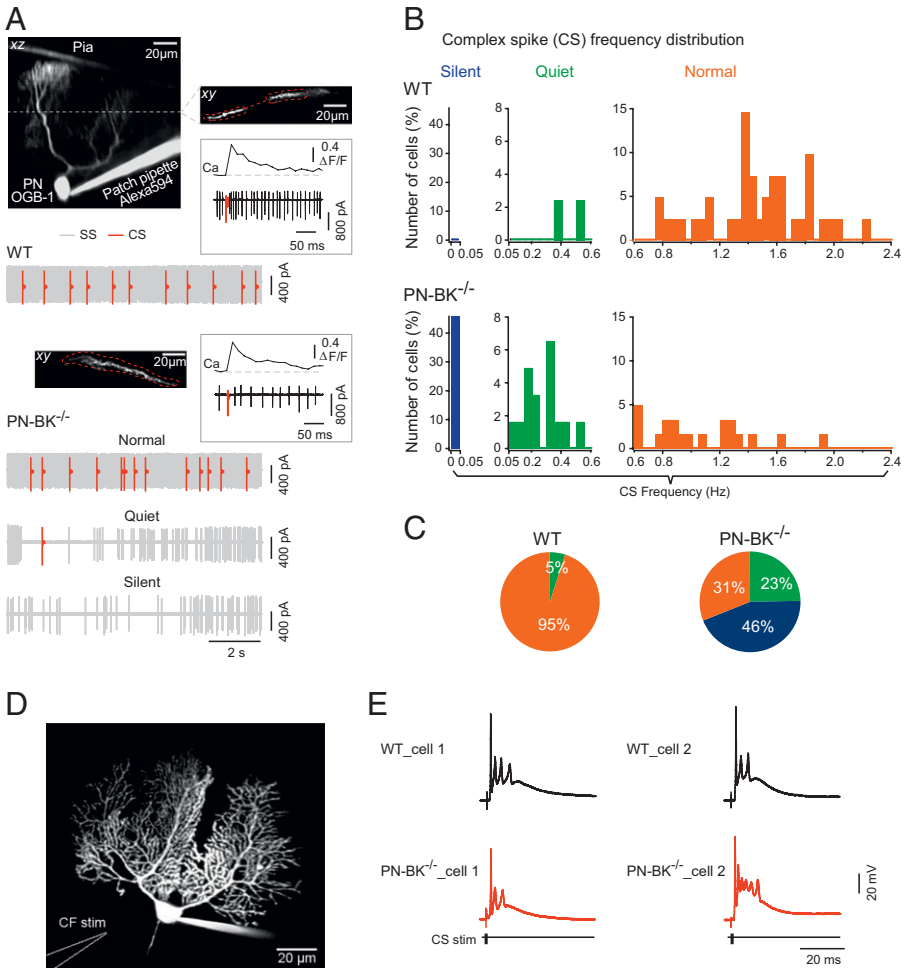

Fig. 2. Silencing of CS activity in PN-BK$^{-/-}$ mice. (*A*) Cell-attached recording and Ca^{2+} imaging of CS activity. Projection images: an electroporated PN filled with Oregon Green BAPTA-1 (OGB-1) from a WT (upper two images) or PN-BK$^{-/-}$ (lower image) mouse. The *xy* image (*Upper Right*) is an optical section through the dendritic tree of the PN at the level marked by the dotted line in the *xz* image (*Upper Left*). Regions of interest are delineated by dotted red lines. *Insets:* Examples of individual CSs and the corresponding Ca^{2+} transients from a WT (*Upper*) or PN-BK$^{-/-}$ (*Lower*) cell. Electrical traces: one example of PN activity in a WT cell and three examples in PN-BK$^{-/-}$ cells. The latter represents the three classes of CS activity: silent (0–0.05 Hz), quiet (0.05–0.6 Hz), and normal (0.6–2.4 Hz). The SS and CS are labeled in gray and red, respectively. The continuous gray background reflects high frequency of SS activity. (*B*) Frequency distribution in the three classes of cells. (*C*) Pie charts summarize the relative proportion of PNs with silent, quiet, or normal climbing fiber activity (n = 34 WT cells and 57 PN-BK$^{-/-}$ cells; 10 mice for each genotype). (*D*) Image of a whole-cell patch-clamped PN and the location of the climbing fiber stimulation pipette (CF stim) in a cerebellar slice preparation. (*E*) Representative traces from two cells of each genotype, showing the characteristic CS waveforms elicited by stimulating the climbing fibers. Note the similarity of the responses (n = 5 WT and 10 PN-BK$^{-/-}$ cells).

change the frequency of CSs (n = 4 cells; $P > 0.05$) (Fig. S5). In the experiment illustrated in Fig. 3*B*, four neighboring PNs of a PN-BK$^{-/-}$ mouse were identified by electroporating them with a fluorescent marker dye. After that, the spiking activity was monitored by sequentially performing cell-attached recordings from each of these PNs. Under control conditions we found that PN2 was silent, that PN1 and PN3 were quiet, and that PN4 was normal (Fig. 3*C*, *Left*). Next, we injected harmaline i.p. Twenty minutes after harmaline injection we performed another round of cell-attached recordings from each of the labeled PN. We found that in all PNs, irrespective of their control status, the CS activity was rescued (Fig. 3*C*). In fact, across the population, the firing frequency of CS in PN-BK$^{-/-}$ mice after harmaline treatment was indistinguishable from that recorded in WT mice (mean CS frequency, 4.0 ± 0.2 Hz for WT and 4.1 ± 0.3 Hz for PN-BK$^{-/-}$; $P > 0.05$; Table S1) (Fig. 3*D*). Next, we examined harmaline-induced tremor (31) in both genotypes. Because this assay requires a normal function of the connection between the IO and the PNs, it serves as a powerful test for the olivo-cerebellar circuit in behaving mice. We found that, as for the harmaline-mediated induction of CS activity in PNs, the tremor behavior was also induced to similar levels in WT and PN-BK$^{-/-}$ mice (n = 7 mice for each genotype; $P > 0.05$) (Fig. 3 *E* and *F*). Thus, our results show that the deletion of BK channels in PNs leads to a massive reduction in the activity of IO neurons, which most likely results from malfunction of the olivo-cerebellar circuit.

To test the role of PN-mediated inhibitory synaptic transmission in the DCN for CS silencing, we designed an in vivo experiment in which we performed cell-attached recordings from PNs while applying $GABA_A$ receptor antagonist (gabazine) or agonist (muscimol) locally to the DCN (Fig. 4 *A* and *B*). The accuracy and the specificity of the drug applications were carefully assessed by coinjecting an inert fluorescent marker dye (Alexa594). The control experiments included the post hoc anatomical verification of the application site (Fig. 4*C*) and the electrophysiological monitoring of the DCN-characteristic neuronal activity through the dye application pipette (Figs. S6 and S7) (see *SI Materials and Methods* for further details). Consistent with the reduced efficacy of the inhibitory synapse between the PN and the DCN neurons in BK$^{-/-}$ mice (2), we observed an increase in firing frequency of DCN neurons in PN-BK$^{-/-}$ mice in vivo. The mean firing frequencies of DCN neurons were 10.5 ± 2.3 Hz in WT mice (n = 16 cells) and 14.7 ± 1.9 Hz in PN-BK$^{-/-}$ mice (n = 14 cells; $P < 0.05$) (Fig. S7). We next applied gabazine to the DCN in WT mice. We found that gabazine application reversibly blocked CS activity (Fig. 4*D*). Additionally, in the other seven PNs tested, gabazine applied to the DCN markedly decreased the CS activity (mean frequency, 1.6 ± 0.1 Hz for control and 0.4 ± 0.2 Hz for gabazine; n = 8 cells; $P < 0.001$; Fig. 4*G*, *Left* and Table S1). This result is reminiscent of earlier findings showing that various manipulations, including local disinhibition in the PN layer, lesions of the DCN, or block of inhibition in the IO, produce an increased frequency of CS activity (32, 33). Together, these results provide strong evidence in support of the hypothesis that PN-mediated inhibition forms one part of the olivo-cerebellar feedback circuit and that climbing fiber activity can be tightly controlled by the inhibitory action from PNs to the DCN. In contrast to gabazine, the $GABA_A$ receptor agonist muscimol had no detectable effect in WT mice (mean frequency, 1.6 ± 0.1 Hz for control and 1.6 ± 0.2 Hz for muscimol; n = 11 cells; $P > 0.05$; Fig. 4*G*, *Right* and Table S1), indicating that under our experimental conditions DCN neurons are nearly

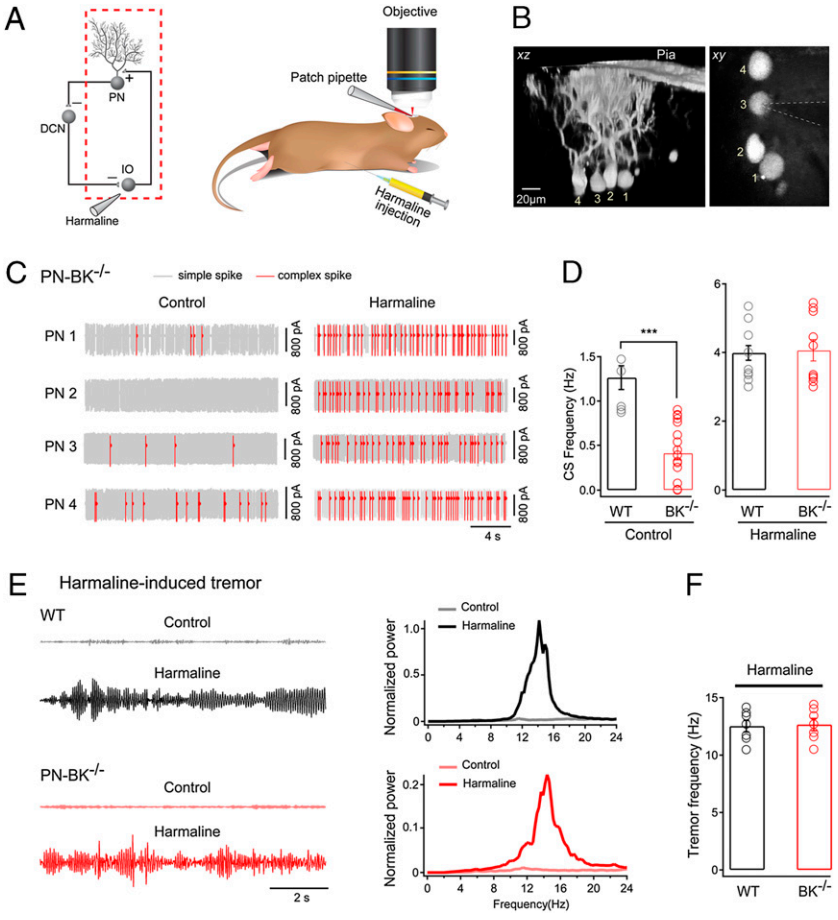

Fig. 3. Rescue of CS activity in PN-BK$^{-/-}$ mice by harmaline. (*A*) Schematic presentation of the olivo-cerebellar circuit (*Left*) and the segment under examination (red dotted square) when harmaline was i.p. injected (*Right*). (*B*) *xz* and *xy* projection images of four electroporated PNs in a PN-BK$^{-/-}$ mouse. The pipette for cell-attached recording is indicated by dotted lines. (*C*) Representative traces recorded before and after harmaline injections from the four PN-BK$^{-/-}$ cells depicted in *B*. Note that the massive increase in CS activity was observed in all PNs in response to harmaline (20 mg/kg). (*D*) Summary of the mean CS frequency from both genotypes in the absence (*Left*) or presence (*Right*) of harmaline (Control: $n = 7$ cells in WT and 18 cells in PN-BK$^{-/-}$; Harmaline: $n = 13$ cells in WT and 10 cells in PN-BK$^{-/-}$; four WT and four PN-BK$^{-/-}$ mice). In the presence of harmaline, the CS frequency in PN-BK$^{-/-}$ mice was similar to that found in WT mice. (*E*) Harmaline-induced tremor in awake, freely moving WT (black) and PN-BK$^{-/-}$ (red) mice. *Left:* Representative tremor-induced force changes recorded by a pressure sensor before and after harmaline injection. *Right:* Normalized power spectra of the force measurements. The major, single peak around 10–15 Hz represents the frequency of harmaline-induced tremor. (*F*) Comparison of the tremor frequency shows no significant difference between WT (12.5 ± 0.5 Hz; $n = 7$) and PN-BK$^{-/-}$ (12.7 ± 0.5 Hz; $n = 7$) mice. ***$P < 0.001$. Error bars show SEM.

maximally inhibited by PN's activity. A critical test of our hypothesis resides in the ability to restore normal CS activity by reestablishing the inhibitory action of PNs on DCN neurons. To that end we applied muscimol to the DCN in PN-BK$^{-/-}$ mice. Fig. 4*F* illustrates such an experiment, in which we recorded a "silent" PN. Application of muscimol reversibly restored a part of the CS activity. A similar rescue, or increase in CS activity, was reliably detected in all PNs tested ($n = 19$; Fig. 4*H* and Table S1). It should be noted that injecting muscimol to the DCN in PN-BK$^{-/-}$ mice is insufficient to entirely restore CS frequency, particularly in silent and quiet cells. The incomplete restoration of the CS activity may be partially due to long-term adaptive changes (e.g., some compensatory mechanisms) in the olivo-cerebellar circuit of PN-BK$^{-/-}$ mice. Alternatively, the focal application of muscimol to a fraction of DCN neurons may be insufficient for a complete restoration of the CS activity. Nevertheless, the rapid and reversible action of muscimol provides direct evidence that the olivo-cerebellar circuit function is dynamically regulated by the level of inhibition within the DCN.

In conclusion, in this study we obtained two major results. First, despite the widespread distribution of BK channels in the brain and particularly in several types of cerebellar neurons (3), we find that the BK channels of PNs are of outstanding importance for the control of motor coordination. In their absence, mice exhibit an ataxic behavior that is reminiscent of that observed in the total BK knockout mice. Second, and most importantly, we demonstrate the functional disruption of the long-range olivo-cerebellar feedback loop in this mouse model of ataxia. Because the deletion of BK channels was restricted to PNs, the malfunction must be the consequence of the altered electrical properties of PNs. Indeed, we found that in PN-BK$^{-/-}$ mice the SS activity was significantly reduced. This relatively mild effect on the SS firing stands in contrast to the robust reduction in CS activity. Moreover, the clear restoration of CS activity by emulating the inhibitory effect of PNs on DCN neurons indicates that the reduced PN-mediated inhibition in the DCN is one of the major sources of the reduced CS activity. It has been reported (2) that in BK$^{-/-}$ mice the efficacy of the inhibitory synapse between the PN and the DCN neurons is markedly reduced, particularly at frequencies higher than 10 Hz. The effective filtering of synaptic transmission at higher frequencies together with the reduced SS activity would serve to strongly attenuate the amount of GABA released from the PN terminals into the DCN. It should be mentioned that a fraction of PNs had a normal CS frequency in PN-BK$^{-/-}$ mice (31%). This indicates that in a subset of olivary neurons the activity was normal, perhaps owing to a reduced efficacy of DCN-mediated inhibition in these neurons. In addition, a minor contribution is expected to arise from the residual expression of BK channels in a small number of PNs (approximately 2–5%), as found previously when using the L7 promotor for the PN-specific deletion of proteins (20, 34). Finally, a hypothetical compensatory mechanism might also contribute to the normal CF activity in a subset of PNs.

Our results provide clear evidence that the anatomical organization of the olivo-cerebellar circuit (17–19), which comprises the cerebellar cortex, the DCN, and the IO, indeed operates as a closed loop. This suggestion is in agreement with recent results of Marshal and Lang (32), demonstrating that experimentally increasing PN firing increases the firing rate and synchrony level of CS. The functional significance of the olivo-cerebellar loop for normal motricity is indicated by the severity of the motor deficits found in our study. The ramification of these findings extends beyond the functional significance of BK channels. It, in fact, identifies a potentially important pathophysiological mechanism for several other forms of cerebellar ataxia. Different types of cerebellar ataxia are characterized by distinct molecular defects that converge into a reduced probability of action potential firing

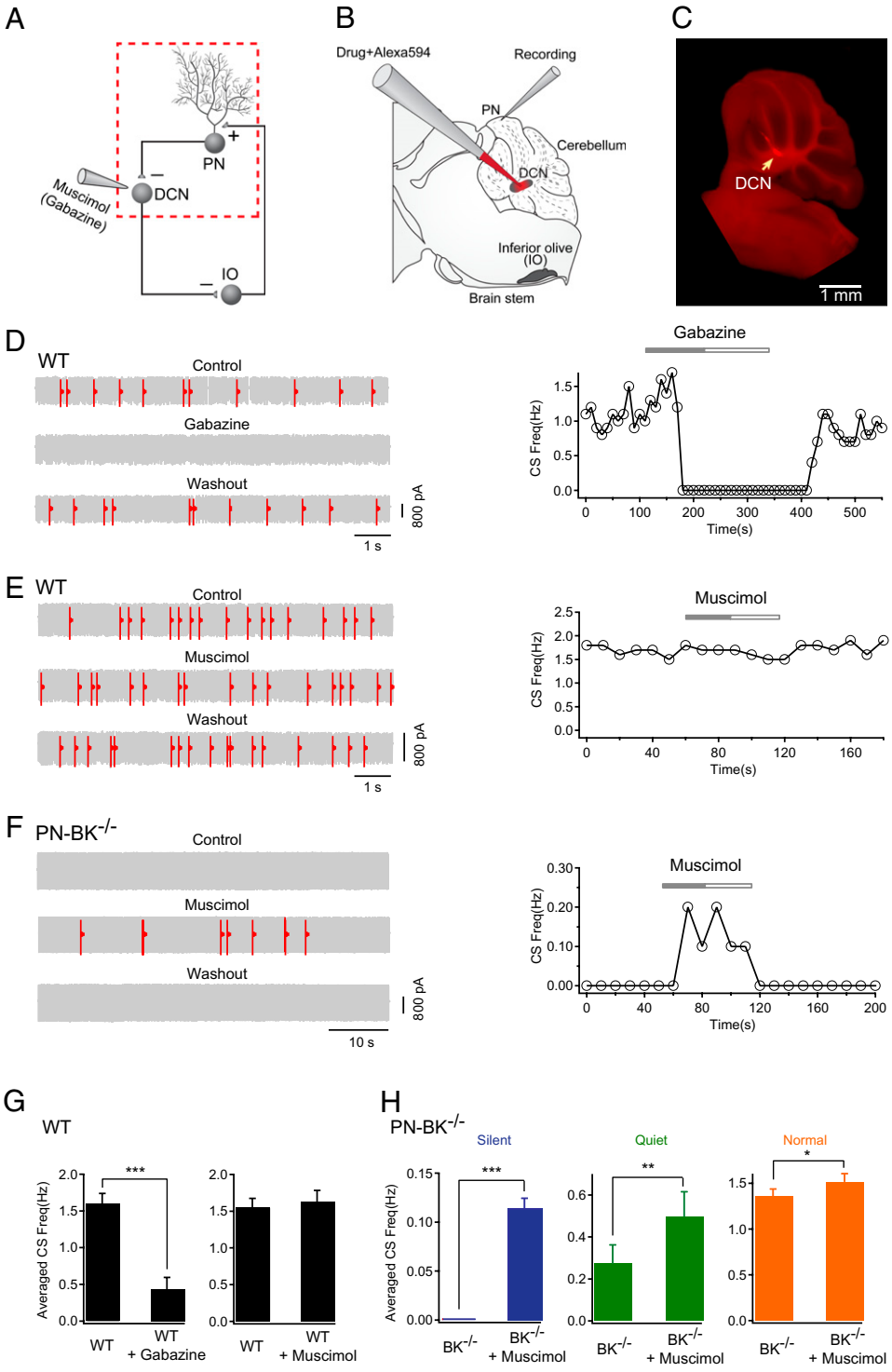

Fig. 4. Rescue of CS activity in PN-BK$^{-/-}$ mice by increasing inhibition in the DCN. (*A*) Schematic presentation of the olivocerebellar circuit (*Left*) and the segment under examination (red dotted square) when gabazine or muscimol was locally applied to the DCN. (*B*) Experimental configuration for cell-attached recordings from PNs and local drug applications to the DCN. The glass pipette for drug application filled with Alexa594 was lowered from cortex into the DCN. (*C*) Fluorescence image showing the site of local drug application within the DCN (arrow). (*D*) Representative electrical traces and time-course of the effect of gabazine on CS activity in a WT cell. Gabazine (200 μM) applied into DCN dramatically reduced the frequency of CS. (*E*) Representative traces and time course showing the absence of effect of muscimol (300 μM) on the CS frequency in a WT mouse. (*F*) The CS activity was restored in a silent PN-BK$^{-/-}$ cell during application of muscimol into DCN. (*G*) Summary of *D* and *E* (n = 8 cells for gabazine experiments, n = 11 cells for muscimol experiments; paired t tests). (*H*) Summary of the effect of muscimol on three classes of CS activity in PN-BK$^{-/-}$ mice: silent (n = 7 cells), quiet (n = 7 cells), and normal (n = 5 cells) (paired t tests). *P < 0.05; **P < 0.01; ***P < 0.001. Error bars show SEM.

in PNs. For example, mice lacking sodium channels $Na_v1.6$ (35) or $Na_v1.1$ (36) channels exhibit ataxia that is associated with an altered depolarizing drive and reduced action potential firing of PNs. In the episodic ataxia type 2 (37) and in the ataxic *tottering* mice (38), a P/Q calcium channel mutation not only leads to a reduced depolarizing drive and a reduced probability of BK channel activation but also to an irregular spike firing and a reduced synaptic transfer to the DCN. Mutation in potassium channels $K_v3.3$ also causes ataxia and results in a defective repolarization of action potentials accompanied by reduced firing rates in PNs (39, 40). Thus, the reduced spike firing at the PN output and the consequently reduced inhibition in the DCN represent a common cellular defect in ataxia. This defect fits with the observation that some forms of ataxia are associated with a selective increase in neuronal firing rates in the DCN (Fig. S7) (13). The present results suggest that in these forms of ataxia, the relatively increased activity of the DCN would lead to an excessive inhibition of the IO. Because this mechanism is independent of the specific etiology, the resultant silencing of CS activity is a likely common motif of these forms of ataxia and may be an important factor in this impairment of cerebellar function.

Materials and Methods

Animals. Adult mice (1–4 months old) were used in all of the experiments. All experimental procedures were performed in accordance with institutional animal welfare guidelines and were approved by the state government of Bavaria, Germany. Details of generation of PN-specific $BK^{-/-}$ mice are given in *SI Materials and Methods*.

Immunohistochemistry of Cerebellar Cortex. The procedure of immunohistochemistry was described previously (3). Additional details are given in *SI Materials and Methods*.

Motor Behavior Tests. Walking behavior tests include footprint pattern test, ladder walking test, and elevated bar balancing test. Additional details are provided in *SI Materials and Methods*.

In Vivo Electrophysiological Recordings. Surgery and in vivo electrophysiological recordings were performed as described previously (41, 42). The recordings were carried out under isoflurane anesthesia. SS and CS from extracellular recordings were sorted according to their amplitudes, shapes, and time courses using Igor Pro (Wavemetrics). Additional details are provided in *SI Materials and Methods*.

In Vitro Electrophysiological Recordings. Parasagittal cerebellar slice preparations and somatic whole-cell recordings were performed as described elsewhere (43). Climbing fiber input was stimulated by placing a patch pipette filled with Ringer solution in the granule layer (0.2 ms, 20–90-V square pulses). The location of the stimulation pipette and the stimulation intensity were adjusted until an all-or-none response was evoked.

Tremor Behavior Measurement. Harmaline-induced tremor was measured using a custom-made sensing device, which is a 13 × 10 × 14-cm plastic box with a pressure sensor (Piezo Electric Pulse Transducer; AD Instruments) underneath the center of the box. The sensor was connected to a PowerLab data acquisition system (AD Instruments), and the signal was filtered by a band pass of 0–24 Hz. Motion activity was recorded digitally and analyzed using Chart 5.0 software (AD Instruments). Each mouse was tested in the box for 10 min before and at least 30 min after i.p. injection of harmaline (20 mg/kg).

Intra-DCN Drug Application. A patch pipette filled with Alexa594 (50 μM) plus muscimol (300 μM) (Sigma) or Alexa594 plus gabazine (200 μM) was lowered from cortex (coordinates: −2.5 mm to Bregma and ±0.36 mm lateral to midline) into the DCN at an angle of 40° (Fig. 4*B*). The resistance of pipette (4–6 MΩ) and extracellular neuronal activity were monitored using an EPC9/2 amplifier with Pulse software (HEKA) during the process of pipette insertion. The location of the DCN was determined by the stereotaxic coordinates (*SI Materials and Methods*) and verified post hoc histologically (Fig. 4*C* and Fig. S6). Drugs and Alexa594 were coapplied locally by pressure injection using a Picospritzer puffer system (Picospritzer III; General Valve) connected to the injection pipette via polyethylene tubing. After completion of experiments, mice were deeply anesthetized by increasing the concentration of isoflurane above 3%, and the injection sites were marked by locally applying Alexa594. Brain slices (400 μm) were then prepared and examined using a fluorescence microscope (Fig. 4*C*).

ACKNOWLEDGMENTS. We thank Jia Lou for excellent technical assistance. This work was supported by the Deutsche Forschungsgemeinschaft (IRTG 1373, SFB 870), the European Research Area (ERA)-Net Program, and the Schiedel Foundation. A.K. is a Carl-von-Linde Senior Fellow of the Institute for Advanced Study of the Technical University Munich.

1. Faber ES, Sah P (2003) Calcium-activated potassium channels: multiple contributions to neuronal function. *Neuroscientist* 9:181–194.
2. Sausbier M, et al. (2004) Cerebellar ataxia and Purkinje cell dysfunction caused by Ca^{2+}-activated K^+ channel deficiency. *Proc Natl Acad Sci USA* 101:9474–9478.
3. Sausbier U, et al. (2006) Ca^{2+} -activated K^+ channels of the BK-type in the mouse brain. *Histochem Cell Biol* 125:725–741.
4. Womack MD, Hoang C, Khodakhah K (2009) Large conductance calcium-activated potassium channels affect both spontaneous firing and intracellular calcium concentration in cerebellar Purkinje neurons. *Neuroscience* 162:989–1000.
5. Womack MD, Khodakhah K (2003) Somatic and dendritic small-conductance calcium-activated potassium channels regulate the output of cerebellar Purkinje neurons. *J Neurosci* 23:2600–2607.
6. Womack MD, Khodakhah K (2002) Characterization of large conductance Ca^{2+}-activated K^+ channels in cerebellar Purkinje neurons. *Eur J Neurosci* 16:1214–1222.
7. Edgerton JR, Reinhart PH (2003) Distinct contributions of small and large conductance Ca^{2+}-activated K^+ channels to rat Purkinje neuron function. *J Physiol* 548:53–69.
8. Gruol DL, Jacquin T, Yool AJ (1991) Single-channel K^+ currents recorded from the somatic and dendritic regions of cerebellar Purkinje neurons in culture. *J Neurosci* 11: 1002–1015.
9. Knaus HG, et al. (1996) Distribution of high-conductance Ca(2+)-activated K+ channels in rat brain: Targeting to axons and nerve terminals. *J Neurosci* 16:955–963.
10. Haghdoost-Yazdi H, Janahmadi M, Behzadi G (2008) Iberiotoxin-sensitive large conductance Ca^{2+} -dependent K^+ (BK) channels regulate the spike configuration in the burst firing of cerebellar Purkinje neurons. *Brain Res* 1212:1–8.
11. Cheron G, et al. (2009) BK channels control cerebellar Purkinje and Golgi cell rhythmicity in vivo. *PLoS ONE* 4:e7991.
12. Orr HT (2004) Into the depths of ataxia. *J Clin Invest* 113:505–507.
13. Shakkottai VG, et al. (2004) Enhanced neuronal excitability in the absence of neurodegeneration induces cerebellar ataxia. *J Clin Invest* 113:582–590.
14. Llinás RR (2009) Inferior olive oscillation as the temporal basis for motricity and oscillatory reset as the basis for motor error correction. *Neuroscience* 162:797–804.
15. Jacobson GA, Rokni D, Yarom Y (2008) A model of the olivo-cerebellar system as a temporal pattern generator. *Trends Neurosci* 31:617–625.
16. Welsh JP, Lang EJ, Suglhara I, Llinás R (1995) Dynamic organization of motor control within the olivocerebellar system. *Nature* 374:453–457.
17. De Zeeuw CI, Berrebi AS (1995) Postsynaptic targets of Purkinje cell terminals in the cerebellar and vestibular nuclei of the rat. *Eur J Neurosci* 7:2322–2333.
18. De Zeeuw CI, Wylie DR, DiGiorgi PL, Simpson JI (1994) Projections of individual Purkinje cells of identified zones in the flocculus to the vestibular and cerebellar nuclei in the rabbit. *J Comp Neurol* 349:428–447.
19. Fredette BJ, Mugnaini E (1991) The GABAergic cerebello-olivary projection in the rat. *Anat Embryol (Berl)* 184:225–243.
20. Barski JJ, Dethleffsen K, Meyer M (2000) Cre recombinase expression in cerebellar Purkinje cells. *Genesis* 28:93–98.
21. Kitamura K, Judkewitz B, Kano M, Denk W, Häusser M (2008) Targeted patch-clamp recordings and single-cell electroporation of unlabeled neurons in vivo. *Nat Methods* 5:61–67.
22. Miall RC, Keating JG, Malkmus M, Thach WT (1998) Simple spike activity predicts occurrence of complex spikes in cerebellar Purkinje cells. *Nat Neurosci* 1:13–15.
23. Murphy JT, Sabah NH (1970) Spontaneous firing of cerebellar Purkinje cells in decerebrate and barbiturate anesthetized cats. *Brain Res* 17:515–519.
24. Häusser M, Clark BA (1997) Tonic synaptic inhibition modulates neuronal output pattern and spatiotemporal synaptic integration. *Neuron* 19:665–678.
25. Loewenstein Y, et al. (2005) Bistability of cerebellar Purkinje cells modulated by sensory stimulation. *Nat Neurosci* 8:202–211.
26. Eccles JC, Llinás R, Sasaki K (1966) The excitatory synaptic action of climbing fibres on the purinje cells of the cerebellum. *J Physiol* 182:268–296.
27. Miyakawa H, Lev-Ram V, Lasser-Ross N, Ross WN (1992) Calcium transients evoked by climbing fiber and parallel fiber synaptic inputs in guinea pig cerebellar Purkinje neurons. *J Neurophysiol* 68:1178–1189.
28. Maejima T, Hashimoto K, Yoshida T, Aiba A, Kano M (2001) Presynaptic inhibition caused by retrograde signal from metabotropic glutamate to cannabinoid receptors. *Neuron* 31:463–475.
29. Konnerth A, Llano I, Armstrong CM (1990) Synaptic currents in cerebellar Purkinje cells. *Proc Natl Acad Sci USA* 87:2662–2665.
30. Zagha E, Lang EJ, Rudy B (2008) Kv3.3 channels at the Purkinje cell soma are necessary for generation of the classical complex spike waveform. *J Neurosci* 28:1291–1300.
31. Llinás R, Volkind RA (1973) The olivo-cerebellar system: Functional properties as revealed by harmaline-induced tremor. *Exp Brain Res* 18:69–87.
32. Marshall SP, Lang EJ (2009) Local changes in the excitability of the cerebellar cortex produce spatially restricted changes in complex spike synchrony. *J Neurosci* 29:14352–14362.
33. Lang EJ, Sugihara I, Llinás R (1996) GABAergic modulation of complex spike activity by the cerebellar nucleoolivary pathway in rat. *J Neurophysiol* 76:255–275.
34. Barski JJ, et al. (2003) Calbindin in cerebellar Purkinje cells is a critical determinant of the precision of motor coordination. *J Neurosci* 23:3469–3477.
35. Levin SI, et al. (2006) Impaired motor function in mice with cell-specific knockout of sodium channel Scn8a (NaV1.6) in cerebellar purkinje neurons and granule cells. *J Neurophysiol* 96:785–793.
36. Kalume F, Yu FH, Westenbroek RE, Scheuer T, Catterall WA (2007) Reduced sodium current in Purkinje neurons from Nav1.1 mutant mice: implications for ataxia in severe myoclonic epilepsy in infancy. *J Neurosci* 27:11065–11074.
37. Walter JT, Alviña K, Womack MD, Chevez C, Khodakhah K (2006) Decreases in the precision of Purkinje cell pacemaking cause cerebellar dysfunction and ataxia. *Nat Neurosci* 9:389–397.
38. Hoebeek FE, et al. (2005) Increased noise level of purkinje cell activities minimizes impact of their modulation during sensorimotor control. *Neuron* 45:953–965.
39. Waters MF, et al. (2006) Mutations in voltage-gated potassium channel KCNC3 cause degenerative and developmental central nervous system phenotypes. *Nat Genet* 38: 447–451.
40. McMahon A, et al. (2004) Allele-dependent changes of olivocerebellar circuit properties in the absence of the voltage-gated potassium channels Kv3.1 and Kv3.3. *Eur J Neurosci* 19:3317–3327.
41. Rochefort NL, et al. (2009) Sparsification of neuronal activity in the visual cortex at eye-opening. *Proc Natl Acad Sci USA* 106:15049–15054.
42. Stosiek C, Garaschuk O, Holthoff K, Konnerth A (2003) In vivo two-photon calcium imaging of neuronal networks. *Proc Natl Acad Sci USA* 100:7319–7324.
43. Takechi H, Eilers J, Konnerth A (1998) A new class of synaptic response involving calcium release in dendritic spines. *Nature* 396:757–760.